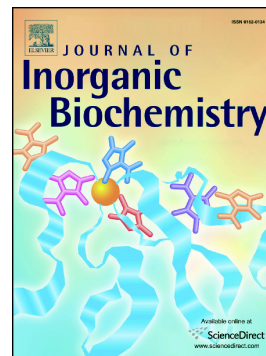


## Journal Pre-proof

Solid-gas reactions for nitroxyl (HNO) generation in the gas phase

Guillermo Carrone, Agostina Mazzeo, Ernesto Marceca, Juan Pellegrino, Sebastián Suárez, Jessica Zarenkiewicz, John P. Toscano, Fabio Doctorovich



PII: S0162-0134(21)00182-3

DOI: <https://doi.org/10.1016/j.jinorgbio.2021.111535>

Reference: JIB 111535

To appear in: *Journal of Inorganic Biochemistry*

Received date: 13 March 2021

Revised date: 1 June 2021

Accepted date: 5 July 2021

Please cite this article as: G. Carrone, A. Mazzeo, E. Marceca, et al., Solid-gas reactions for nitroxyl (HNO) generation in the gas phase, *Journal of Inorganic Biochemistry* (2018), <https://doi.org/10.1016/j.jinorgbio.2021.111535>

This is a PDF file of an article that has undergone enhancements after acceptance, such as the addition of a cover page and metadata, and formatting for readability, but it is not yet the definitive version of record. This version will undergo additional copyediting, typesetting and review before it is published in its final form, but we are providing this version to give early visibility of the article. Please note that, during the production process, errors may be discovered which could affect the content, and all legal disclaimers that apply to the journal pertain.

© 2018 © 2021 Published by Elsevier Inc.

## Solid-gas reactions for nitroxyl (HNO) generation in the gas phase

Guillermo Carrone<sup>a,1</sup>, Agustina Mazzeo<sup>a,1</sup>, Ernesto Marceca<sup>a</sup>, Juan Pellegrino<sup>a</sup>,  
Sebastián Suárez<sup>a</sup>, Jessica Zarenkiewicz<sup>b</sup>, John P. Toscano<sup>b</sup>, and Fabio Doctorovich<sup>a,\*</sup>

<sup>a</sup>Departamento de Química Inorgánica, Analítica, y Química Física, Facultad de Ciencias Exactas y Naturales, Universidad de Buenos Aires, INQUIMAE-CONICET, Ciudad Universitaria, Pab. 2, C1428EHA Buenos Aires, Argentina.

<sup>b</sup>Department of Chemistry, Johns Hopkins University, Baltimore, Maryland 21218, United States

### Abstract

A novel nitroxyl (HNO) generation method is presented, which consists of the reaction between a gaseous base and an HNO donor in the solid phase, allowing the formation of gaseous HNO in a fast and economical way. This method avoids the need of using a liquid system or extreme experimental conditions, and allows to obtain HNO directly in the gas phase for medical use or other applications.

### Keywords

Nitroxyl, HNO, gaseous, Piloty's Acid

### Introduction

Nitroxyl (azanone, HNO) is an inorganic small molecule, widely studied due to its high biological significance.<sup>1,2</sup> HNO is an expected intermediate in biochemical pathways,<sup>3,4</sup> and has reported medical applications regarding its

---

<sup>1</sup>These authors contributed equally.

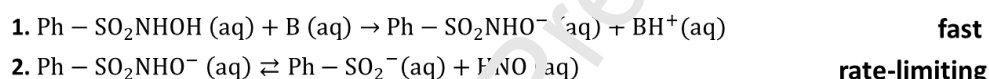
cardioprotective action.<sup>5-7</sup> This highly reactive species has been found to exert beneficial physiological effects, some of its own, and some overlapping with those of NO.<sup>8-10</sup> The medical use of HNO as an agent to prevent cardiac arrest,<sup>2</sup> as a vasodilator<sup>11</sup> and as an antibacterial agent<sup>12</sup> is being developed by the use of HNO donors in solution, which allow more controlled generation. Once formed, HNO readily reacts towards biological targets and itself, dimerizing to yield nitrous oxide (N<sub>2</sub>O) and water.<sup>13</sup>

The first HNO donor, Angeli's salt (Na<sub>2</sub>N<sub>2</sub>O<sub>3</sub>)<sup>14</sup> is still widely used in biological experiments. Since then, several HNO donor compounds have been developed.<sup>15</sup> An important set of compounds, known as Pictet's acid (PA) derivatives,<sup>16-19</sup> act as HNO donors in a two-step mechanism involving fast deprotonation of the sulfohydroxamic moiety followed by slow nitroxyl release. (Scheme 1). The rate of HNO formation depends on each derivative's pK<sub>a</sub>, which exhibit a range between -1 and 9 in aqueous solution, influenced by the ring substitution pattern.<sup>16-19</sup> PA and its derivatives have been used as HNO donors in different reactions, mostly in aqueous solution.<sup>20,21</sup> Only a few employ a non-liquid phase as a solvent, requiring extreme conditions, such as high temperatures.<sup>22-24</sup> The search for new HNO generation methods is of great interest and the possibility of performing the reaction with no liquid phases emerges as a new and promising strategy for the use of gaseous HNO in chemical or medical applications. Moreover, developing a system for the controlled generation of gaseous HNO may allow for the study of its reactivity in the gas phase, such as its reaction towards molecular oxygen. Some controversy remains in this regard, since both peroxynitrite and NO· + HO<sub>2</sub>· have been proposed as possible products in solution.<sup>25-28</sup> Due to further reactivity of the proposed products, the study of these

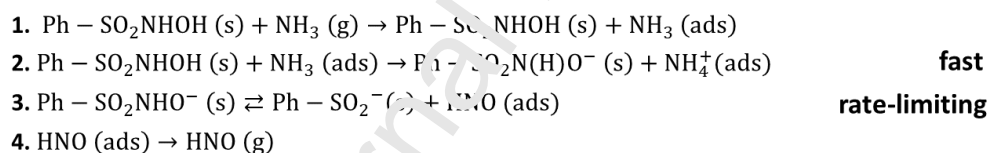
systems has not been an easy task.<sup>1,8</sup> We studied the reaction of solid Piloty's acids derivatives with a gaseous base (e.g., NH<sub>3</sub> (g)). The results showed that this method is an easy and economical way to generate HNO without the need for liquid phases or extreme experimental conditions. Similar studies with another base-catalyzed HNO donor, a (hydroxylamino)pyrazolone (HAPY) derivative, demonstrate the generality of this approach.

Scheme 1. Mechanism of HNO generation in aqueous solution (a), proposed heterogeneous (solid-gas) reaction path (b), and nitroxyl dimerization and dehydration (c)

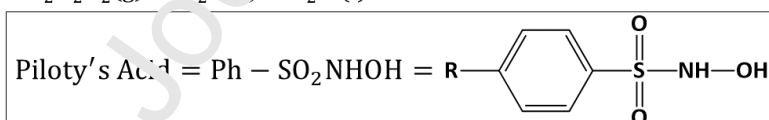
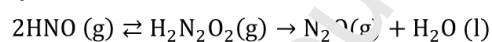
#### a) HNO generation in aqueous solution



#### b) Heterogeneous HNO generation



#### c) HNO dimerization



## Materials and methods

Commercially available reagents from Sigma Aldrich were used as received.

Piloty's acid derivatives N-hydroxy-4-nitrobenzenesulfonamide (NO<sub>2</sub>-PA) and N-hydroxy-4-fluorobenzenesulfonamide (F-PA) were synthesized from the corresponding benzene-sulfonyl chloride and hydroxylamine hydrochloride in the

presence of MgO, according to literature methods.<sup>19</sup> The products were further purified using a silica gel chromatography column as reported independently.<sup>29</sup>

4-(N-Hydroxylamino)-4-(acetyl-O-methoxyoxime)-N-phenyl-3-

methylpyrazolone (HAPY-1) was synthesized according to literature procedure.<sup>30</sup>

The identity and purity of the resulting compounds were monitored by <sup>1</sup>H NMR spectroscopy. Ammonia was generated by adding NH<sub>4</sub>OH solution to sodium hydroxide pellets in a sealed evacuated flask. Gas was allowed to evolve until the reaction became less vigorous. The amount of gaseous water present in the flask following this procedure was estimated to be < 3% in moles in our experimental conditions (298K, 1 atm). Since gaseous water does not react with NO<sub>2</sub>-PA, the observed results are exclusively due to reaction with NH<sub>3</sub>(g).

### **NMR spectroscopy**

<sup>1</sup>H NMR spectroscopy measurements were carried out using a BRUKER Avance Neo 500 MHz spectrometer using d<sub>6</sub>-DMSO purchased from Sigma Aldrich as a solvent.

### **IR measurements**

IR measurements were made with a Thermo Nicolet Avatar 320 FT-IR spectrometer, using a five-centimeter-long gas cell with NaCl windows. In a standard experiment, approximately 3.5 mg of PA derivative were placed each time inside the mounted cell which was afterwards purged with a continuous argon flow and sealed with septa. For each experiment, approximately 15-20 ml gaseous NH<sub>3</sub> in the flask were extracted with a syringe and injected into the IR

cell. 8-scan measurements were continuously made until transmittance changes were no longer observed.

### **Electrochemical HNO detection**

HNO detection was also carried out with a previously described method based on a three-electrode system consisting of platinum counter electrode, Ag/AgCl reference electrode, and a gold working electrode modified with a cobalt porphyrin covalently attached via a 1-decanethiol moiety.<sup>31,32</sup> The method has been demonstrated to be specific for HNO, showing no interference or spurious signal due to the presence of NO, O<sub>2</sub>, NO<sub>2</sub><sup>-</sup>, and other RNOS.<sup>31,32</sup>

### **MS measurements**

#### Procedure #1

Gaseous products developed from solid NO<sub>2</sub>-PA in the presence of 100 mbar of anhydrous ammonia were identified on-line using a capillary-based interface to a high-pressure (1-1000 mbar) Leybold Topatron-B radiofrequency mass spectrometer (MS). The setup (see Supporting Information) consists of a 0.5 cm<sup>3</sup> stainless steel reaction vessel that is continuously sampled with the mass analyzer. The vessel containing the NO<sub>2</sub>-PA powder is connected to an ancillary gas handling system, through which gaseous NH<sub>3</sub> is put in contact with the solid.

A combination of a metering valve and a very narrow capillary is used to fine adjust the flow sampled by the MS. The temperature of the vessel and MS interface is adjusted to 90 °C during the experiments. The low internal volume of the interface region provides a response time of less than 15 seconds, while a

complete mass spectrum is recorded in less than 10 seconds. The data is constantly acquired in a digital oscilloscope.

Gaseous products generated in the reaction of an aqueous solution containing 10 mM of NO<sub>2</sub>-PA, at pH = 10, were analyzed by the same MS procedure in order to validate the detection (and fragmentation) of the product N<sub>2</sub>O.

### Procedure #2

Products from the reaction of solid NO<sub>2</sub>-PA and NH<sub>3</sub> (g) were also monitored using a Hiden EI mass spectrometer.<sup>33</sup> NO<sub>2</sub>-PA (10 mg) or HAPY-1 (10 mg) was placed into a 25 mL glass reaction vessel which was evacuated with a vacuum pump. The reaction vessel was connected to the mass spectrometer through a fused silica capillary (0.10 mm ID, 25 ft) and 10 mL of anhydrous NH<sub>3</sub> (g) from AirGas was injected into the reaction vessel using a 10 mL gas tight syringe to initiate the reaction. The rate of NH<sub>3</sub> addition was controlled by using a programmable syringe pump. Products were monitored for 25 minutes with continuous sampling.

### **Results and discussion**

When solid *N*-hydroxy-4-nitrobenzenesulfonamide (NO<sub>2</sub>-PA) is exposed to gaseous ammonia (50:1 molar ratio), its color turns from pale yellow to orange, and N<sub>2</sub>O evolution is observed by gas-phase IR spectroscopy. After injecting the gaseous base inside the IR cell containing NO<sub>2</sub>-PA, the characteristic N<sub>2</sub>O signal (2250-2150 cm<sup>-1</sup>) was monitored,<sup>35</sup> and its intensity was found to increase with time (Figure 1). Full spectra for one of the experiments can be found in Section S1.

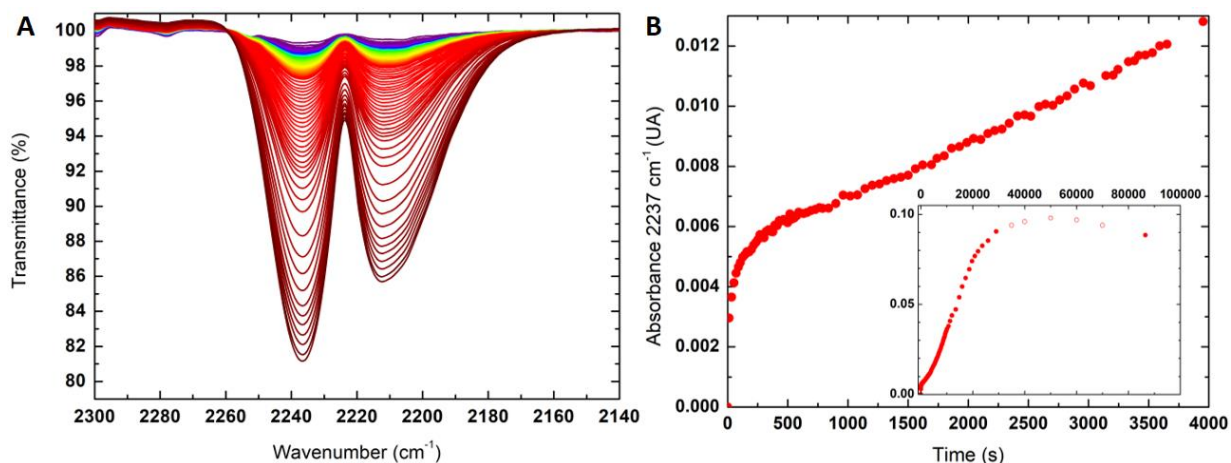


Figure 1. A) FT-IR spectral changes observed in the region corresponding to the characteristic N<sub>2</sub>O signal during the reaction of solid NO<sub>2</sub>-FA with gaseous ammonia. B) Experimental absorbance at 2237 cm<sup>-1</sup> (N<sub>2</sub>O signal) as a function of time, corresponding to the spectral changes observed in Figure 1, during the first 4000 seconds. Process 1 ( $k_0$ ) behaviour is observed at short timescales followed by a linear response (Process 2, order 0,  $k_{RXN}$ ). Inset: full experiment, lasting over 27 h

Absorbance traces, shown in Figure 1B, indicate two different processes over relatively short timescales: an induction period, evidenced by a fast growth of the N<sub>2</sub>O signal following a first-order process, and a few minutes later, a linear dependence of the signal as a function of time, indicating a zero-order kinetic process. A possible explanation for this behavior might be that the N<sub>2</sub>O signal growth experimentally observed during the first seconds is dependent on the rate of NH<sub>3</sub> adsorption and on the efficiency of the gas phase mixing and diffusion process (Process 1,  $k_0$ ). A second process begins when an equilibrium NH<sub>3</sub> concentration is reached over the surface of the solid, and so the concentration of N<sub>2</sub>O grows linearly as a function of time (zero-order regime, Process 2,  $k_{RXN}$ ), until reactive sites begin to become scarce. For more details, see section S2 in SI. Other IR experiments and kinetic fittings are shown in section S3 in the SI.



Since in the present reaction  $\text{N}_2\text{O}$  is produced by HNO dimerization,<sup>13</sup> the degree of  $\text{N}_2\text{O}$  generation,  $\alpha\text{P}$ , was calculated as a function of time using the IR spectroscopy measurements at  $2237\text{ cm}^{-1}$  and compared to theoretical values, resulting in a first order kinetic regime (Figure 1B, section S2 in SI). The calculated rate constant ( $k$ ) associated with the first process was equal to  $k_0 = (7 \pm 2) \times 10^{-2}\text{ s}^{-1}$ . The rate constant for the second (linear) process ( $k_{\text{RXN}}$ ) is ca.  $10^{-8}\text{ M}\cdot\text{s}^{-1}$ . There is a large error for the rate constant associated with this second process, because its rate likely depends on particle size, porosity, and other factors (see below and SI).

Since HNO's dimerization rate is faster than its production, as already described for aqueous solution,<sup>15,36</sup> it is possible to follow the production of HNO as a function of  $\alpha\text{P}$  of the dimerization byproduct,  $\text{N}_2\text{O}$ . Scheme 1 shows the mechanism of HNO generation from PA in aqueous solution (a), a plausible reaction path for the heterogeneous (solid-gas) reaction studied in this work (b), and the dimerization and dehydration reaction of HNO (c) ( $k_{\text{DIM}} = 8 \times 10^6\text{ M}^{-1}\text{s}^{-1}$  in aqueous solution, estimated between  $0.5$  and  $1.6 \times 10^6\text{ M}^{-1}\text{s}^{-1}$  in the gas phase)<sup>37</sup>. Likewise, if the deprotonation rate of solid PA (Scheme 1, Eq. b2) is greater than the generation rate of HNO (Scheme 1, Eq. b3), the latter reaction will be the limiting step of the overall production of HNO, together with the surface kinetics described before. The first-order rate constant  $k_0$  obtained for the formation of HNO from  $\text{NO}_2\text{-PA (s)} + \text{NH}_3\text{ (g)}$  during the first few minutes of the reaction is surprisingly similar to the one obtained for  $\text{NO}_2\text{-PA (aq)}$  in basic solution ( $4.4 \times 10^{-2}\text{ s}^{-1}$ ,  $\text{pH} = 10$ ,  $T = 298\text{ K}$ ),<sup>16-21</sup> and faster than the rate constant obtained at  $\text{pH} 5$ .<sup>16-21,36</sup>

The N<sub>2</sub>O production yield reached an approximate value of 25% ± 2% from FT-IR measurements (see section S4 in SI). An independent <sup>1</sup>H-NMR experiment showed that ca. 65% of the initial amount of NO<sub>2</sub>-PA was still unreacted. The ca. 10% difference in the expected N<sub>2</sub>O yield (25% versus ca. 35% of NO<sub>2</sub>-PA that has reacted) can be attributed to some N<sub>2</sub>O loss by unexpected leaks.<sup>25-27</sup> The relatively small N<sub>2</sub>O yield suggests that gaseous ammonia readily reacts with the surface of the solid, with little diffusion inside the particles, so that most solid remains unreactive. Crushing the solid with a mortar and pestle did not produce a noticeable increase on the reaction rate or total N<sub>2</sub>O yield, presumably because this process only decreased aggregation (see section S3 in SI), not resulting in a net increase of available surface sites. In fact, a small decrease was observed in the reaction rate, indicating that the solid particles were probably more compact after crushing. The complete set of calculated constants is shown in Table S1. N<sub>2</sub>O generation was also observed by using gaseous triethylamine as the base. Reaction of NH<sub>3</sub> and another PA derivative, *N*-hydroxy-4-fluorobenzenesulfonamide (F-PA), was also followed by IR spectroscopy, showing the same behavior observed at short timescales. For more details, see SI. We have also found some preliminary evidence that NH<sub>3</sub> could directly react with HNO in the gas phase, explaining the relative low amounts of N<sub>2</sub>O formed in these experiments. This will be studied carefully in an upcoming work.

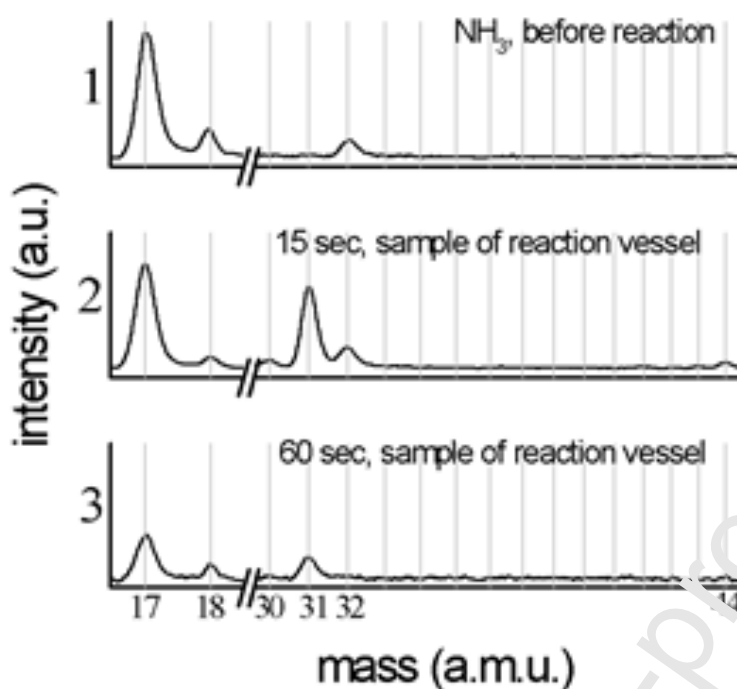


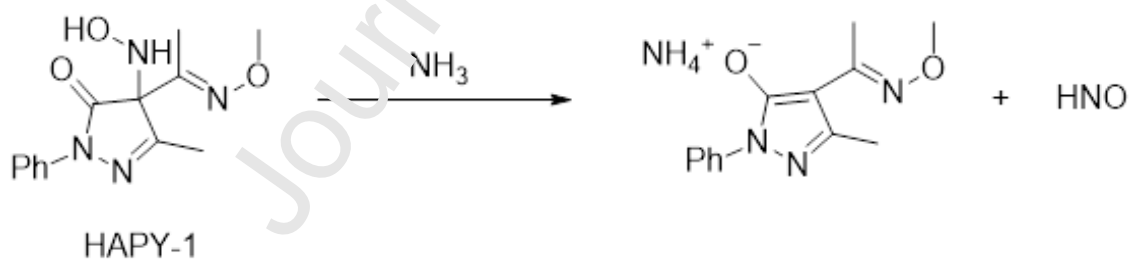
Figure 2. Representative mass spectra recorded along the reaction of solid NO<sub>2</sub>-PA and gaseous ammonia at 90 °C. Panels: (1) gaseous NH<sub>3</sub> before reaction, (2) reaction mixture at  $t = 15$  s, (3) reaction mixture at  $t = 60$  s.

The reaction was also followed by mass spectrometry (MS) using two different methods. For details, see section S8 in SI. In the first case, the gaseous products developed in the reaction were identified on-line using a high-pressure (1-1000 mbar) radiofrequency mass spectrometer (Procedure #1). Figure 2 shows a series of representative mass spectra taken during a typical experiment. The mass spectrum depicted in the upper panel was obtained by sampling 100 mbar of gaseous ammonia, before allowing contact with the NO<sub>2</sub>-PA solid. The main signal results from the NH<sub>3</sub><sup>+</sup> molecular ion ( $m/z$  17), while smaller peaks at  $m/z$  18 (H<sub>2</sub>O<sup>+</sup>) and 32 (O<sub>2</sub><sup>+</sup>) reflect that some moisture and air were incorporated in the system during the injection. The spectrum in the next panel was taken

approximately 15 seconds after the reaction started ( $t = 0$ ), maintaining the temperature at 90 °C. Interestingly, clear evidence of the formation of  $\text{HNO}^+$  is visible (molecular ion at  $m/z$  31). A careful inspection of spectrum 2 in Figure 2 allows one to recognize two very small signals accounting for  $\text{N}_2\text{O}^+$  ( $m/z$  44) and the fragmentation product  $\text{NO}^+$  ( $m/z$  30) which can arise from  $\text{N}_2\text{O}$  or  $\text{HNO}$ . At this point, peaks from  $\text{H}_2\text{O}$  and  $\text{O}_2$  present in the spectrometer have decreased due to pumping. The third spectrum, sampled one minute after the reaction started, reflects the situation in which the reaction leading to  $\text{HNO}$  is elapsed and, consequently, the  $\text{HNO}^+$  signal at  $m/z$  31 drops as a result of pumping, while those at  $m/z$  30 ( $\text{NO}^+$ ) and 44 ( $\text{N}_2\text{O}^+$ ) are only barely visible. The intense signals observed for  $\text{HNO}^+$  in Figure 2, especially in spectra 2, indicates that under our experimental conditions  $\text{HNO}$  dimerization is relatively slow in comparison with the same reaction in water, probably due to the absence of a solvent cage. Moreover, low pressure conditions in the reaction vessel and the manifold decrease the encounter probability of two  $\text{HNO}$  molecules.

To validate the new MS method discussed above, the reaction was also followed by EI-MS using Procedure #2 (Figure 3), which is described in the SI. With this method, masses  $m/z$  30 ( $\text{NO}^+$ ), 31 ( $\text{HNO}^+$  or  $^{15}\text{NO}^+$ ) and 44 ( $\text{N}_2\text{O}^+$ ) were monitored in positive ion mode. Mixing of  $\text{NH}_3$  (g) and  $\text{NO}_2$ -PA results in an increase in all three of these signals. The  $m/z$  31 signal can arise from either  $\text{HNO}$  generation or from the naturally abundant  $^{15}\text{NO}^+$  fragment of  $\text{N}_2\text{O}$ .<sup>38,39</sup> From a series of  $\text{N}_2\text{O}$  control experiments, the ratio of  $m/z$  30 to  $m/z$  31 from  $^{15}\text{NO}^+$  is determined to be 255( $\pm$ 3):1. A ratio smaller than 255:1 is, therefore, evidence for  $\text{HNO}$  generation. From the reaction of solid  $\text{NO}_2$ -PA with anhydrous  $\text{NH}_3$  (g), the observed  $m/z$  30 to 31 ratio is 35 ( $\pm$ 8):1 after considering possible contributions

to the  $m/z$  30 signal from the  $\text{NH}_3$  source (see section S8B in SI). This corresponds to an  $m/z$  31 signal that is approximately 85%  $\text{HNO}^+$  while the other 15% is attributed to  $^{15}\text{NO}^+$ . Small amounts of  $\text{N}_2\text{O}$  are also generated as a result of HNO dimerization. We varied the rate of  $\text{NH}_3$  injection from 5 mL/min (Figure 3A) to 2 mL/min (Figure 3B) and found that this led to a slower observed release of HNO. The  $m/z$  30 to 31 ratio was not changed by varying the rate of  $\text{NH}_3$  addition. To examine if this reaction is possible with other base-catalyzed HNO donors, HAPY-1, a pyrazalone based HNO donor,<sup>40</sup> was also incubated with  $\text{NH}_3$  under the same conditions (Scheme 2, Figure S15). HNO release was also confirmed from the reaction of HAPY-1 with  $\text{NH}_3$  with an observed  $m/z$  30 to 31 ratio of 50 ( $\pm 9$ ):1 (see section S8 in SI). This corresponds to an  $m/z$  31 signal that is approximately 80%  $\text{HNO}^+$  and 20%  $^{15}\text{NO}^+$ . While these donors have different half lives in solution, both donors released HNO at the same rate under these conditions based on the rate of  $\text{NH}_3$  addition.



Scheme 2. Generation of HNO from HAPY-1

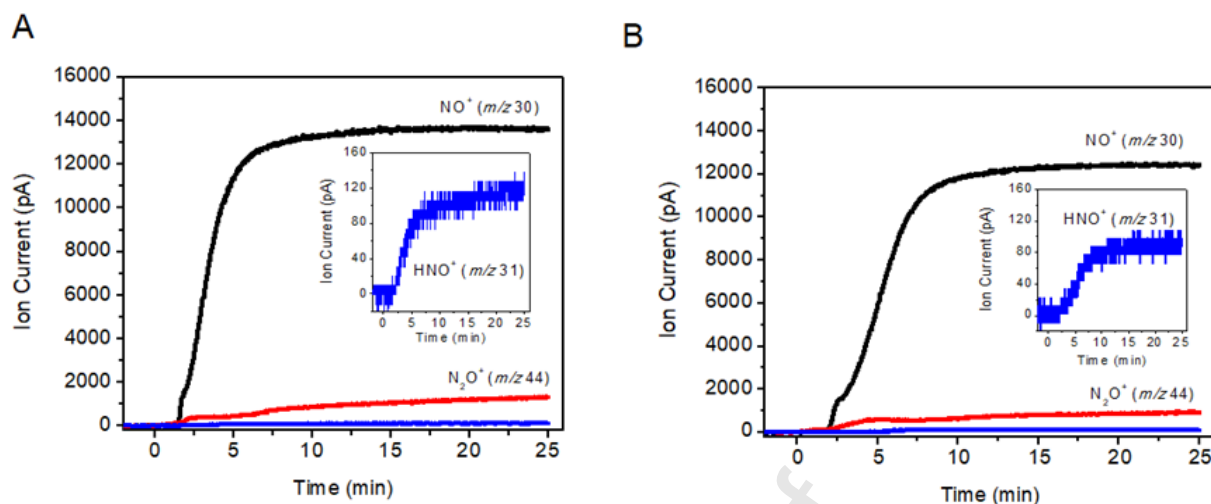


Figure 3. Mass spectrum recorded from the reaction of  $\text{NO}_2\text{-TA}$  and anhydrous  $\text{NH}_3$  (g) at RT by Procedure #2. Accounting for contribution to the  $m/z$  30 signal from the  $\text{NH}_3$  (g) source, a ratio of  $m/z$  30 to 31 of  $35 (\pm 8):1$  confirms the generation of HNO in this reaction. A)  $\text{NH}_3$  added at a rate of 5 mL/min and B)  $\text{NH}_3$  added at a rate of 2 mL/min

A much more intense HNO signal ( $m/z$  31) is observed in the case of Procedure #1. This is likely due to the higher temperature applied to the reaction, less HNO dilution, and a wider capillary used in the case of Procedure #1. For more details, see section S8 in SI.

To confirm the MS results indicating gaseous HNO generation, a trapping experiment using a selective electrochemical HNO sensor<sup>31,32</sup> was performed in aqueous solution, verifying its production from the gas-solid reaction (see section S9 in SI).

## Conclusions

Results show that gaseous HNO can be generated through a heterogeneous phase reaction without the need of extreme experimental conditions. Heating of the reaction mixture, combined with gas dilution and a fast flow, minimize the production of  $\text{N}_2\text{O}$  by HNO dimerization, making it feasible to administer a gas containing HNO as the main species, as observed by MS (Procedure #1).

This opens the gate for the study of new methods to achieve direct generation of this elusive molecule. From the MS experiments, HNO generation appears to be dependent on the rate of  $\text{NH}_3$  administration rather than on the lifetime of donors in an aqueous solution, at least for the PA and HAPY donors examined (i.e., it could be possible to control the rate by the gaseous base administration rate). Preliminary experiments were also performed in a similar way to explore the reactivity of solid Angeli's salt, an acid-catalysed HNO donor, with gaseous HCl, resulting in  $\text{N}_2\text{O}$  production via FT-IR and MS Procedure #1. This reaction will be further explored soon.

This simple and controlled generation of gaseous HNO may provide a new drug delivery scheme to be implemented in novel medical treatments. NO inhalation can reduce the need of assisted ventilation in conditions such as pneumonia or other acute respiratory syndromes,<sup>44-45</sup> and so the therapeutic administration of gaseous HNO is worth studying. In this regard, although the presence of  $\text{NH}_3$  (or HCl) can be disadvantageous due to potential toxicity, diverse methods could be engineered to eliminate the gaseous base (or acid) from the system. Some possibilities might include trapping the excess base (or acid) by using a membrane, or an appropriate aqueous solution.<sup>46,47</sup>

### **Funding**

The research reported in this publication was supported by the Ministerio de Ciencia, Tecnología e Innovación Productiva (PICT-2015-3854 and PICT-2017-1930) and the Universidad de Buenos Aires (UBACYT) project # 20020170100595BA. Funding was also provided to JPT by the US National Science Foundation (CHE-1900285).

### **Conflicts of interest**

There are no conflicts to declare.

#### Author statement

**Guillermo Carrone: Investigation, Methodology, Formal Analysis** **Agostina Mazzeo: Investigation, Formal Analysis, Visualization, Writing – Original Draft and Editing** **Ernesto Marceca: Methodology, Formal Analysis, Validation** **Juan Pellegrino: Investigation, Writing – Review and Editing** **Sebastián Suárez: Investigation, Formal Analysis** **Jessica Zarenkiewicz: Investigation, Formal Analysis, Validation** **John Toscano: Methodology, Validation, Formal Analysis, Funding acquisition** **Fabio Doctorovich: Conceptualization, Funding acquisition, Supervision**

#### Declaration of interests

The authors declare that they have no known competing financial interests or personal relationships that could have appeared to influence the work reported in this paper.

#### References

- (1) Doctorovich, F.; Farmer, P. J.; Martí, M. A. *The Chemistry and Biology of Nitroxyl (HNO)*; Elsevier, 2016, Vol. 53. <https://doi.org/10.1016/c2013-0-18854-x>.
- (2) Fukuto, J. M. A Recent History of Nitroxyl Chemistry, Pharmacology and Therapeutic Potential. *British Journal of Pharmacology* **2019**, *176* (2), 135–146. <https://doi.org/10.1111/bph.14384>.
- (3) Doctorovich, F.; Piekal, D. E.; Pellegrino, J.; Suárez, S. A.; Martí, M. A. Reactions of HNO with Metal Porphyrins: Underscoring the Biological Relevance of HNO. *Accounts of Chemical Research* **2014**, *47* (10), 2907–2916. <https://doi.org/10.1021/ar500153c>.
- (4) Flores-Santana, W.; Salmon, D. J.; Donzelli, S.; Switzer, C. H.; Basudhar, D.; Ridnour, L.; Cheng, R.; Glynn, S. A.; Paolucci, N.; Fukuto, J. M.; Miranda, K. M.; Wink, D. A. The Specificity of Nitroxyl Chemistry Is Unique Among Nitrogen Oxides in Biological Systems. *Antioxidants & Redox Signaling* **2011**, *14* (9), 1659–1674. <https://doi.org/10.1089/ars.2010.3841>.
- (5) Tocchetti, C. G.; Wang, W.; Froehlich, J. P.; Huke, S.; Aon, M. A.; Wilson, G. M.; Di Benedetto, G.; O'Rourke, B.; Gao, W. D.; Wink, D. A.; Toscano, J. P.; Zaccolo, M.; Bers, D. M.; Valdivia, H. H.; Cheng, H.; Kass, D. A.; Paolucci, N. Nitroxyl Improves Cellular Heart Function by Directly Enhancing Cardiac Sarcoplasmic Reticulum Ca<sup>2+</sup> Cycling. *Circulation Research* **2007**, *100* (1), 96–104. <https://doi.org/10.1161/01.RES.0000253904.53601.c9>.
- (6) Guo, Y.; Xu, J.; Wu, L.; Deng, Y.; Wang, J.; An, J. Advances in Research on Treatment of Heart Failure with Nitrosyl Hydrogen. *Heart Failure Reviews* **2019**, *24* (6), 941–948. <https://doi.org/10.1007/s10741-019-09800-6>.



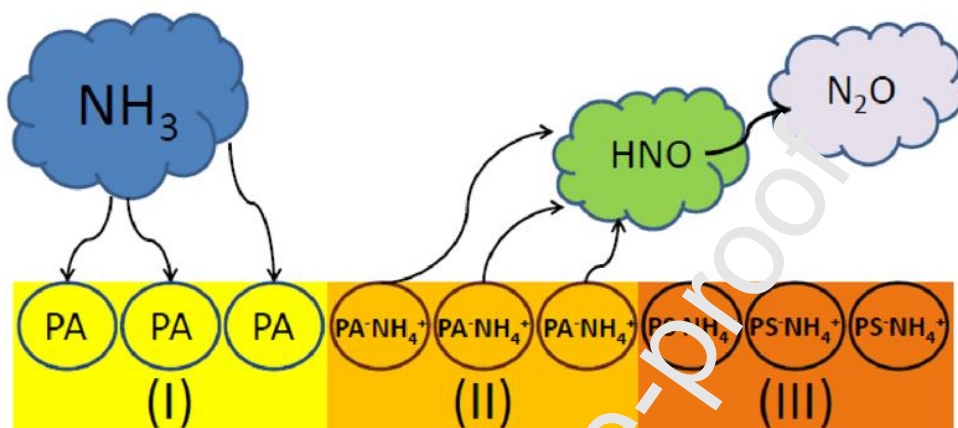
- (7) Sun, H.-J.; Wu, Z.-Y.; Cao, L.; Zhu, M.-Y.; Nie, X.-W.; Huang, D.-J.; Sun, M.-T.; Bian, J.-S. Role of Nitroxyl (HNO) in Cardiovascular System: From Biochemistry to Pharmacology. *Pharmacological Research* **2020**, *159*, 104961. <https://doi.org/10.1016/j.phrs.2020.104961>.
- (8) Suarez, S. A.; Vargas, P.; Doctorovich, F. Updating NO•/HNO Interconversion under Physiological Conditions: A Biological Implication Overview. *J. Inorg. Biochem.* **2020**.
- (9) Ma, X. L.; Gao, F.; Liu, G.-L. L.; Lopez, B. L.; Christopher, T. A.; Fukuto, J. M.; Wink, D. A.; Feelisch, M. Opposite Effects of Nitric Oxide and Nitroxyl on Postischemic Myocardial Injury. *Proceedings of the National Academy of Sciences* **1999**, *96* (25), 14617–14622. <https://doi.org/10.1073/pnas.96.25.14617>.
- (10) Miranda, K. M.; Paolucci, N.; Katori, T.; Thomas, D. D.; Ford, E.; Bartberger, M. D.; Espey, M. G.; Kass, D. A.; Feelisch, M.; Fukuto, J. M.; Wink, D. A. A Biochemical Rationale for the Discrete Behavior of Nitroxyl and Nitric Oxide in the Cardiovascular System. *Proceedings of the National Academy of Sciences* **2003**, *100* (16), 9196–9201. <https://doi.org/10.1073/pnas.1430507100>.
- (11) Velagic, A.; Qin, C.; Woodman, O. L.; Horowitz, J. D.; Ritchie, R. H.; Kemp-Harper, B. K. Nitroxyl: A Novel Strategy to Circumvent Diabetes Associated Impairments in Nitric Oxide Signaling. *Frontiers in Pharmacology* **2020**, *11*. <https://doi.org/10.3389/fphar.2020.00727>.
- (12) Galizia, J.; Acosta, M. P.; Urdániz, E.; Martí, M. A.; Piuri, M. Evaluation of Nitroxyl Donors' Effect on Mycobacteria. *Tuberculosis* **2018**, *109*, 35–40. <https://doi.org/10.1016/j.tube.2018.01.005>.
- (13) Shafirovich, V.; Lyman, S. V. Nitroxyl and Its Anion in Aqueous Solutions: Spin States, Protic Equilibria, and Reactivities toward Oxygen and Nitric Oxide. *Proceedings of the National Academy of Sciences of the United States of America* **2002**, *99* (11), 7340–7345. <https://doi.org/10.1073/pnas.112202099>.
- (14) Angeli, A. Sopra La Nitroironoammina. *Gazz. Chim. Ital.* **1896**, *26*, 17–25.
- (15) Basudhar, D.; Bharadwaj, G.; Salmon, D. J.; Miranda, K. M. HNO Donors. In *The Chemistry and Biology of Nitroxyl (HNO)*; Elsevier, 2017; pp 11–36. <https://doi.org/10.1016/B978-0-12-800934-5.00002-5>.
- (16) Adas, S. K.; Bharadwaj, V.; Zhou, Y.; Zhang, J.; Seed, A. J.; Brasch, N. E.; Sampson, P. Synthesis and HNO Donating Properties of the Piloty's Acid Analogue Trifluoromethanesulphonylhydroxamic Acid: Evidence for Quantitative Release of HNO at Neutral PH Conditions. *Chemistry – A European Journal* **2018**, *24* (29), 7330–7334. <https://doi.org/10.1002/chem.201800662>.
- (17) Smulik-Izydorczyk, R.; Rostkowski, M.; Gerbich, A.; Jarmoc, D.; Adamus, J.; Leszczyńska, A.; Michalski, R.; Marcinek, A.; Kramkowski, K.; Sikora, A. Decomposition of Piloty's Acid Derivatives – Toward the Understanding of Factors Controlling HNO Release. *Archives of Biochemistry and Biophysics* **2019**, *661*, 132–144. <https://doi.org/10.1016/j.abb.2018.11.012>.
- (18) Sirsalmath, K.; Suárez, S. A.; Bikiel, D. E.; Doctorovich, F. The PH of HNO Donation Is Modulated by Ring Substituents in Piloty's Acid Derivatives: Azanone Donors at Biological PH. *Journal of Inorganic Biochemistry* **2013**, *118*, 134–139. <https://doi.org/10.1016/j.jinorgbio.2012.10.008>.
- (19) Porcheddu, A.; De Luca, L.; Giacomelli, G. A Straightforward Route to Piloty's Acid Derivatives: A Class of Potential Nitroxyl-Generating Prodrugs. *Synlett* **2009**, *2009* (13), 2149–2153. <https://doi.org/10.1055/s-0029-1217565>.

- (20) Carrone, G.; Pellegrino, J.; Doctorovich, F. Rapid Generation of HNO Induced by Visible Light. *Chemical Communications* **2017**, 53 (38), 5314–5317. <https://doi.org/10.1039/C7CC02186K>.
- (21) Toscano, J. P.; Brookfield, F. A.; GB; Cohen, A. D.; Courtney, S. M.; Frost, L. M.; Kalish, V. J. United States Patent: 10487049 - N-Hydroxylsulfonamide Derivatives as New Physiologically Useful Nitroxyl Donors. 10487049, 2019.
- (22) Harteck, P. Die Darstellung von HNO Bzw. [HNO] n. *Berichte der deutschen chemischen Gesellschaft (A and B Series)* **1933**, 66 (3), 423–426. <https://doi.org/10.1002/cber.19330660325>.
- (23) Clyne, M. A. A.; Thrush, B. A. Reaction of Nitrogen Dioxide with Active Nitrogen. *Transactions of the Faraday Society* **1961**, 57, 69. <https://doi.org/10.1039/tf9615700069>.
- (24) Clyne, M. A. A.; Thrush, B. A. Mechanism of Chemiluminescent Reactions Involving Nitric Oxide—the H + NO Reaction. *Discussions Faraday Soc.* **1962**, 33, 139–148. <https://doi.org/10.1039/DF9623300139>.
- (25) Fukuto, J. M.; Hobbs, A. J.; Ignarro, L. J. Conversion of Nitroxyl (HNO) to Nitric Oxide (NO) in Biological Systems: The Role of Physiological Oxidants and Relevance to the Biological Activity of HNO. *Biochemical and Biophysical Research Communications* **1993**, 196 (2), 707–713. <https://doi.org/10.1006/bbrc.1993.2307>.
- (26) Smulik, R.; Dębski, D.; Zielonka, J.; Michałowicz, B.; Adamus, J.; Marcinek, A.; Kalyanaraman, B.; Sikora, A. Nitroxyl (HNO) Reacts with Molecular Oxygen and Forms Peroxynitrite at Physiological pH. *Journal of Biological Chemistry* **2014**, 289 (51), 35570–35581. <https://doi.org/10.1074/jbc.M114.597740>.
- (27) Chazotte-Aubert, L.; Oikawa, S.; Calibert, I.; Bianchini, F.; Kawanishi, S.; Ohshima, H. Cytotoxicity and Site-Specific DNA Damage Induced by Nitroxyl Anion (NO<sup>-</sup>) in the Presence of Hydrogen Peroxide. *Journal of Biological Chemistry* **1999**, 274 (30), 20909–20915. <https://doi.org/10.1074/jbc.274.30.20909>.
- (28) Miranda, K. M.; Dutton, A. J.; Ridnour, L. a; Foreman, C. a; Ford, E.; Paolocci, N.; Katori, T.; Tocchetti, C. G.; Mancardi, D.; Thomas, D. D.; Espey, M. G.; Houk, K. N.; Fukuto, J. M.; Wink, D. a. Mechanism of Aerobic Decomposition of Angeli's Salt (Sodium Trioxodinitrate) at Physiological PH. *Journal of the American Chemical Society* **2005**, 127 (2), 722–731. <https://doi.org/10.1021/ja045480z>.
- (29) Aizawa, K.; Nakagawa, H.; Matsuo, K.; Kawai, K.; Ieda, N.; Suzuki, T.; Miyata, N. Piloty's Acid Derivative with Improved Nitroxyl-Releasing Characteristics. *Bioorganic & Medicinal Chemistry Letters* **2013**, 23 (8), 2340–2343. <https://doi.org/10.1016/j.bmcl.2013.02.062>.
- (30) Guthrie, D. A.; Ho, A.; Takahashi, C. G.; Collins, A.; Morris, M.; Toscano, J. P. “Catch-and-Release” of HNO with Pyrazolones. *The Journal of Organic Chemistry* **2015**, 80 (3), 1338–1348. <https://doi.org/10.1021/jo502330w>.
- (31) Suárez, S. A.; Bikiel, D. E.; Wetzler, D. E.; Martí, M. A.; Doctorovich, F. Time-Resolved Electrochemical Quantification of Azanone (HNO) at Low Nanomolar Level. *Analytical Chemistry* **2013**, 85 (21), 10262–10269. <https://doi.org/10.1021/ac402134b>.
- (32) Doctorovich, F.; Suárez, S. A.; Martí, M. A.; Battaglini, F. International Patent “HNO Biosensor”, WO2020/136414 A1, 2018.
- (33) Cline, M. R.; Tu, C.; Silverman, D. N.; Toscano, J. P. Detection of Nitroxyl (HNO) by Membrane Inlet Mass Spectrometry. *Free Radical Biology and*

- Medicine* **2011**, *50* (10), 1274–1279.  
<https://doi.org/10.1016/j.freeradbiomed.2011.02.008>.
- (34) Neese, F. The ORCA Program System. *Wiley Interdiscip. Rev.: Comput. Mol. Sci.* **2012**, *2*, 73–78.
- (35) Heinecke, J. L.; Khin, C.; Pereira, J. C. M.; Suárez, S. A.; Iretskii, A. V.; Doctorovich, F.; Ford, P. C. Nitrite Reduction Mediated by Heme Models. Routes to NO and HNO? *Journal of the American Chemical Society* **2013**, *135* (10), 4007–4017. <https://doi.org/10.1021/ja312092x>.
- (36) Bonner, F. T.; Ko, Y. Kinetic, Isotopic, and Nitrogen-15 NMR Study of N-Hydroxybenzenesulfonamide Decomposition: An Nitrosyl Hydride (HNO) Source Reaction. *Inorganic Chemistry* **1992**, *31* (12), 2514–2519.  
<https://doi.org/10.1021/ic00038a038>.
- (37) Fehling, C.; Friedrichs, G. Dimerization of HNO in Aqueous Solution: An Interplay of Solvation Effects, Fast Acid-Base Equilibria, and Intramolecular Hydrogen Bonding? *Journal of the American Chemical Society* **2011**, *133* (44), 17912–17922. <https://doi.org/10.1021/ja2075949>.
- (38) Cline, M. R.; Tu, C.; Silverman, D. N.; Toscano, J. P. Detection of Nitroxyl (HNO) by Membrane Inlet Mass Spectrometry. *Free Radical Biology and Medicine* **2011**, *50* (10), 1274–1279.  
<https://doi.org/10.1016/j.freeradbiomed.2011.02.008>.
- (39) Chavez, T. A.; Toscano, J. P. Detection of HNO by Membrane Inlet Mass Spectrometry. In *The Chemistry and Biology of Nitroxyl (HNO)*; Doctorovich, F., Farmer, P. J., Martí, M. A., Eds.; Elsevier: 2017; pp 255–267.  
<https://doi.org/10.1016/B978-0-12-800934-5.00013-X>.
- (40) Basceken, S.; Balci, M. Design of Pyrazolo-Pyrrolo-Pyrazines and Pyrazolo-Pyrrolo-Diazepines via AuCl<sub>3</sub>-Catalyzed and NaH-Supported Cyclization of N-Propargyl Pyrazoles. *J. Org. Chem.* **2015**, *80* (8), 3806–3814.  
<https://doi.org/10.1021/acs.joc.5b00034>.
- (41) Madjid, M.; Casscells, S. W. Of Birds and Men: Cardiologists' Role in Influenza Pandemics. *The Lancet* **2004**, *364* (9442), 1309. [https://doi.org/10.1016/S0140-6736\(04\)17176-6](https://doi.org/10.1016/S0140-6736(04)17176-6).
- (42) Vetta, F.; Vetta, G.; Mannaccio, L. Coronavirus Disease 2019 (COVID-19) and Cardiovascular Disease: A Vicious Circle. *Journal of Cardiology and Cardiovascular Research* **2020**, *1* (2), 1–12.
- (43) Kobayashi, J.; Murata, I. Nitric Oxide Inhalation as an Interventional Rescue Therapy for COVID-19-Induced Acute Respiratory Distress Syndrome. *Annals of Intensive Care* **2020**, *10* (1), 61. <https://doi.org/10.1186/s13613-020-00681-9>.
- (44) Martel, J.; Ko, Y.-F.; Young, J. D.; Ojcius, D. M. Could Nasal Nitric Oxide Help to Mitigate the Severity of COVID-19? *Microbes and Infection* **2020**.  
<https://doi.org/10.1016/j.micinf.2020.05.002>.
- (45) Monsalve-Naharro, J. Á.; Domingo-Chiva, E.; Castillo, S. G.; Cuesta-Montero, P.; Jiménez-Vizueté, J. M. Inhaled Nitric Oxide in Adult Patients with Acute Respiratory Distress Syndrome. *Farmacia Hospitalaria*. 2017, pp 292–312.  
<https://doi.org/10.7399/fh.2017.41.2.10533>.
- (46) Wang, P.; Chung, T.-S. Recent Advances in Membrane Distillation Processes: Membrane Development, Configuration Design and Application Exploring. *Journal of Membrane Science* **2015**, *474*, 39–56.  
<https://doi.org/10.1016/j.memsci.2014.09.016>.

- (47) EL-Bourawi, M. S.; Khayet, M.; Ma, R.; Ding, Z.; Li, Z.; Zhang, X. Application of Vacuum Membrane Distillation for Ammonia Removal. *Journal of Membrane Science* **2007**, *301* (1–2), 200–209. <https://doi.org/10.1016/j.memsci.2007.06.021>.

### Graphical Abstract



### Highlights

- A novel method for  $\text{HNO}$  production in the gas phase is described.
- The method consists of heterogeneous reactions between solid  $\text{HNO}$  donors and gaseous  $\text{NH}_3$ .
- This method can be useful for chemical studies and medical applications.